Supporting Information

Mononuclear (*O,O′* or *N,N′*) and Heterodinuclear (*O,O′* and *N,N′*) Transition-Metal Complexes of *ortho*-Quinoid Bis(pyrazol-1-yl)methane Ligands

Florian Blasberg, Michael Bolte, Hans-Wolfram Lerner, and Matthias Wagner

Content:

1. NMR-Spectroscopic Data of 6 in C_6D_6; Synthesis and Analytical Data of 8, 13, and 15.

NMR-Spectroscopic Data of 6. ^{1}H-NMR (300.0 MHz, C_6D_6) δ = 1.29 (s, 18 H; *t*Bu-CH_3), 5.92 (d, $^3J_{HH}$ = 2.5 Hz, 2 H; pz-H4), 6.16 (ddd, $^3J_{HH}$ = 8.2 Hz, $^4J_{HH}$ = 2.2 Hz, $^4J_{HH}$ = 0.7 Hz, 1H; HQ-H6), 6.37 (dd, $^4J_{HH}$ = 2.2 Hz, $^4J_{HH}$ = 0.4 Hz, 1 H; HQ-H2), 6.48 (d, $^3J_{HH}$ = 8.2 Hz, 1 H; HQ-H5), 6.97 (d, $^3J_{HH}$ = 2.5 Hz, 2 H; pz-H5), 7.53 (n.r., 1 H; CH). ^{13}C-NMR (75.4 MHz, C_6D_6) δ = 30.7 (*t*Bu-CH_3), 32.5 (*t*Bu-*C*CH_3), 78.0 (Cpz_2), 103.0 (pz-C4), 113.5, 115.6, 119.8 (HQ-C2,5,6), 130.0 (pz-C5), 145.7, 146.1 (HQ-C3,4), 163.4 (pz-C3), n.o. HQ-C1.

Synthesis of 8. A solution of CAN (0.45 g, 0.814 mmol) in MeCN/H_2O (2:1, 3 mL) was added at room temperature to a solution of **6** (0.10 g, 0.27 mmol) and 4-*t*Bu-pyridine (0.20 mL, 0.19 g, 1.40 mmol) in MeCN (5 mL). After the resulting dark solution had been stirred for 75 min, more H_2O (10 mL) was added. The mixture was extracted with CH_2Cl_2 (3 × 5 mL) and the CH_2Cl_2 extracts were discarded. Upon slow evaporation of the residual liquid phase, colorless needles of **8** separated, which were suitable for X-ray crystal structure determination. ESI-MS: *m*/*z* (%) = 504 $[M–NO_3]^+$ (77), 565 $[M−H]^−$ (84), 628 $[M+NO_3]^−$ (14).

Synthesis of 13. Following the general procedure outlined for the synthesis of **11**, **6** (80 mg, 0.217 mmol) was treated with Tl*O*t*Bu (120 mg, 0.434 mmol) and $[(ppy)_2IrCl]_2$ (116 mg, 0.109 mmol) in THF (3.0 mL) to yield a red solid. Yield: 215 mg (92%). Some ^{1}H-NMR signals are poorly resolved due to the presence of two isomers with very similar chemical shift values. An unambiguous assignment of the signals to the individual isomers is not possible. ^{1}H-NMR (300.0 MHz, d^8-THF) δ = 1.23, 1.24 (2 × s, 2 × 18 H; 2 × *t*Bu-CH_3), 5.66 (dd, $^3J_{HH}$ = 8.0 Hz, $^4J_{HH}$ = 1.8 Hz, 2 H; HQ-H6), 5.99, 6.01 (2 × d, 2 × $^3J_{HH}$ = 2.4 Hz, 2 × 2 H; 2 × pz-H4), 6.21 (m, 4 H; ppy-H), 6.30 (m, 4 H; HQ-H2,5), 6.45, 6.68 (2 × m, 2 × 4 H; 2 × ppy-H), 6.90, 6.98 (2 × m, 2 × 2 H; 2 × ppy-H), 7.08 (m, 4 H; pz-H5), 7.21 (s, 2 H; CH), 7.41, 7.62, 7.79, 8.86 (4 × m, 4 × 4 H; 4 × ppy-H). The two different isomers lead to two sets of ^{13}C NMR signals with very similar chemical shift values; in some cases, not all signals are resolved so that the number of resonances listed does not equal twice the number of C atoms. ^{13}C-NMR (75.4 MHz, d^8-THF) δ = 31.2 (*t*Bu-CH_3), 32.9 (*t*Bu-*C*CH_3), 79.8, 79.9 (Cpz_2), 101.9, 102.0 (pz-C4), 114.9 (HQ-C6), 116.1, 116.6 (HQ-C2,5), 119.1, 121.1, 121.3, 122.6, 122.8, 124.7, 124.8 (4 × ppy-C), 127.5 (HQ-C1), 129.6, 129.7 (ppy-C), 129.9, 130.1 (pz-C5), 135.3, 137.2, 137.3, 146.9, 147.0, 149.5, 151.9 (5 × ppy-C), 162.1, 162.2 (pz-C3), 168.7, 169.0 (HQ-C3,4) n.o. ppy-C1. λ_{max}/nm (ε) 370 (26500), 445 (15100), 517 (6100). ESI-MS: *m*/*z* (%) = 867 $[M–Tl]^−$ (46). Anal. Calcd for $C_{43}H_{42}IrN_6O_2Tl$ [1071.43]: C 48.20, H 3.95, N 7.84. Found: C 47.64, H 4.43, N 7.29.

Synthesis of 15. Following the representative procedure outlined for the synthesis of **11**, **6** (100 mg, 0.271 mmol) was reacted with Tl*O*t*Bu (151 mg, 0.543 mmol) and $[(Cp^*)IrCl_2]_2$ (108 mg, 0.135 mmol) in THF (3.0 mL) to yield a bright red solid. Yield: 188 mg (quant.). Single crystals were grown by gas-phase diffusion of pentane into a THF solution of **13**. ^{1}H-NMR (300.0 MHz, d^8-THF) δ = 1.25 (s, 18 H; *t*Bu-CH_3), 1.87 (s, 15 H; Cp*-CH_3), 6.07 (d, $^3J_{HH}$ = 2.4 Hz, 1 H; pz-H4), 6.21 (ddd, $^3J_{HH}$ = 8.2 Hz, $^4J_{HH}$ = 2.0 Hz, $^4J_{HH}$ = 0.6 Hz, 1 H; HQ-H6), 6.48 (d, $^4J_{HH}$ = 2.0 Hz, 1 H; HQ-H2), 6.75 (d, $^3J_{HH}$ = 8.2 Hz, 1 H; HQ-H5), 7.30 (d, $^3J_{HH}$ = 2.4 Hz; pz-H5), 7.49 (n.r., 1 H; CH). ^{13}C-NMR (75.4 MHz, d^8-THF) δ = 10.2 (Cp*-*C*H_3), 31.7 (*t*Bu-CH_3), 32.8 (*t*Bu-*C*CH_3), 79.1 (Cpz_2), 85.0 (Cp*), 102.2 (pz-C4), 113.5 (HQ-C2), 114.1 (HQ-C5), 117.3 (HQ-C6), 127.7 (HQ-C1), 130.1 (pz-C5), 162.2 (pz-C3), 165.0, 165.6 (HQ-C3,4). λ_{max}/nm (ε) 287 (19600), 425 (36500). ESI-MS: *m*/*z* (%) = 735 $[M+MeCN+H]^+$ (33). Anal. Calcd for $C_{31}H_{41}IrN_4O_2$ [693.90]: C 53.66, H 5.96, N 8.07. Found: C 53.40, H 5.85, N 7.95.

2. X-ray Crystal Structure Analysis of 8, 11, and 15.

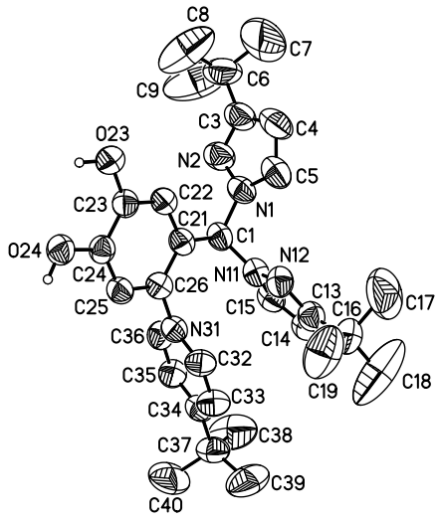

Figure 1S. Molecular structure of the cationic portion of **8** (50% displacement ellipsoids; H-atoms, except for OH groups, omitted for clarity). Selected bond lengths [Å], bond angles [°], torsion angles [°], and dihedral angles [°]: C1−N1 1.466(5), C1−N11 1.453(5), C1−C21 1.519(5), C23−O23 1.355(5), C24−O24 1.365(5), C26−N31 1.465(5); C21−C1−N1 111.5(3), C21−C1−N11 112.7(3), C21−C26−N31 121.7(3), C26−N31−C32 120.1(3), N1−C1−N11 109.7(3); C21−C1−N1−N2 −85.9(4), C21−C1−N11−N12 −51.1(5), C21−C26−N31−C32 104.1(4); HQ//pz(N1) 86.0, HQ//pz(N11) 79.6, HQ//py(N31) 77.3, pz(N1)//pz(N11) 56.4.

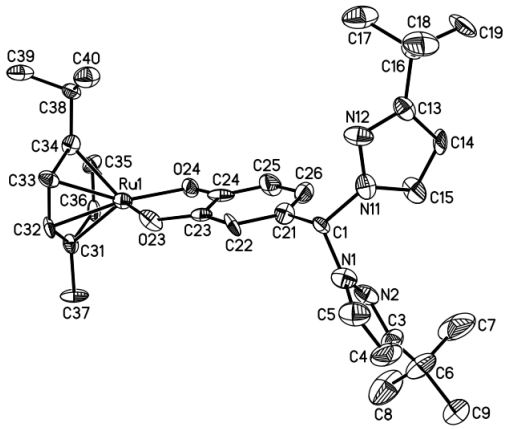

Figure 2S. Molecular structure of the ruthenium complex **11** (50% displacement ellipsoids, H-atoms omitted for clarity). Selected bond lengths [Å], bond angle [°], and dihedral angles [°]: Ru1−O23 1.965(9), Ru1−O24 1.964(8), Ru1···COG(*p*-cym) 1.65, C23−O23 1.356(14), C24−O24 1.326(15); O23−Ru1−O24 80.2(4); HQ//pz(N1) 63.7, HQ//pz(N11) 86.0, pz(N1)//pz(N11) 74.0.

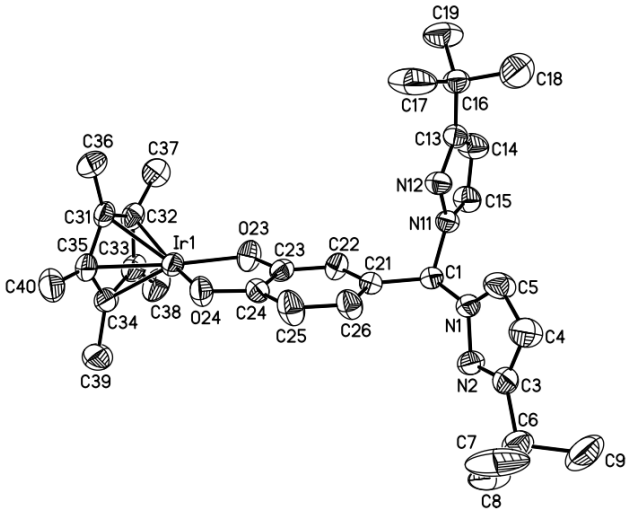

Figure 3S. Molecular structure of **15** (50% displacement ellipsoids, H-atoms omitted for clarity). Selected bond lengths [Å], bond angle [°], and dihedral angles [°]: Ir1−O23 1.993(3), Ir1−O24 1.987(3), Ir1···COG(Cp*) 1.76, C23−O23 1.347(5), C24−O24 1.360(5); O23−Ir1−O24 81.0(1); HQ//pz(N1) 80.7, HQ//pz(N11) 88.5, pz(N1)//pz(N11) 57.8.

Table 1S. Crystallographic Data of **8**, **11**, and **15**.

Compound	**8**	**11**	**15**
formula	$[C_{30}H_{40}N_5O_2][NO_3] \times 1.5\ H_2O$	$C_{31}H_{40}N_4O_2Ru$	$C_{31}H_{41}IrN_4O_2$
fw	591.70	601.74	693.88
color, shape	colorless plate	red/green plate	orange block
temp (K)	193(2)	173(2)	173(2)
radiation	CuK_α, 1.54178 Å	MoK_α, 0.71073 Å	MoK_α, 0.71073 Å
crystal system	tetragonal	monoclinic	orthorhombic
space group	$I4_1/a$	$P2_1/c$	*Pbca*
a (Å)	34.6611(4)	19.6707(19)	10.4679(3)
b (Å)	34.6611(4)	12.5604(15)	21.7161(11)
c (Å)	22.3350(3)	11.856(3)	26.6018(10)
α (deg)	90.00	90.00	90.00
β (deg)	90.00	94.787(13)	90.00
γ (deg)	90.00	90.00	90.00
V (Å^3)	26833.1(6)	2919.1(9)	6047.2(4)
Z	32	4	8
$D_{calcd.}$ (g cm^{-3})	1.172	1.369	1.524
F(000)	10144	1256	2784
μ (mm^{-1})	0.684	0.571	4.448
cryst size (mm)	0.50 × 0.26 × 0.07	0.10 × 0.05 × 0.03	0.35 × 0.27 × 0.25
no of rflns coll	244174	27438	24531
no of indep rflns (R_{int})	11025 (0.1571)	5131 (0.3382)	5870 (0.0463)
data / restr /params	11025 / 0 / 770	5131 / 0 / 344	5870 / 0 / 377
GOOF on F^2	1.533	0.747	1.015
*R*1, *wR*2 ($I>2\ \sigma(I)$)	0.1109, 0.3432	0.0737, 0.1248	0.0339, 0.0805
*R*1, *wR*2 (all data)	0.1308, 0.3694	0.2010, 0.1716	0.0471, 0.0857
largest diff peak and hole (e Å^{-3})	1.531, −0.607	0.943, −0.794	0.892, −1.388

3. Cyclic Voltammetry on 6, 14, and 16.

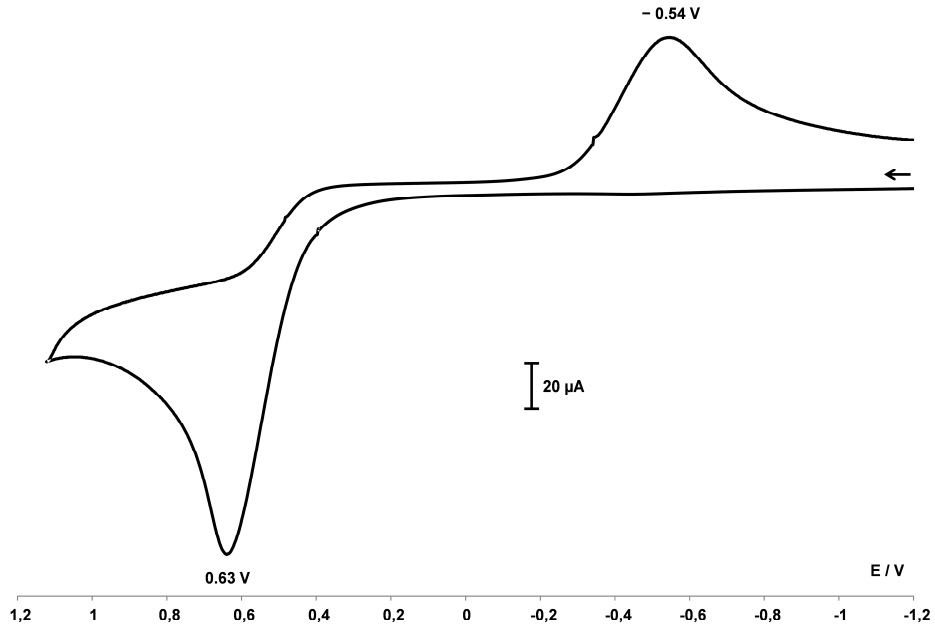

Figure 4S: Cyclic voltammogram of **6** (DMF, 0.1 M $[Bu_4N][PF_6]$, vs. FcH/FcH^+, 200 mV s^{-1}).

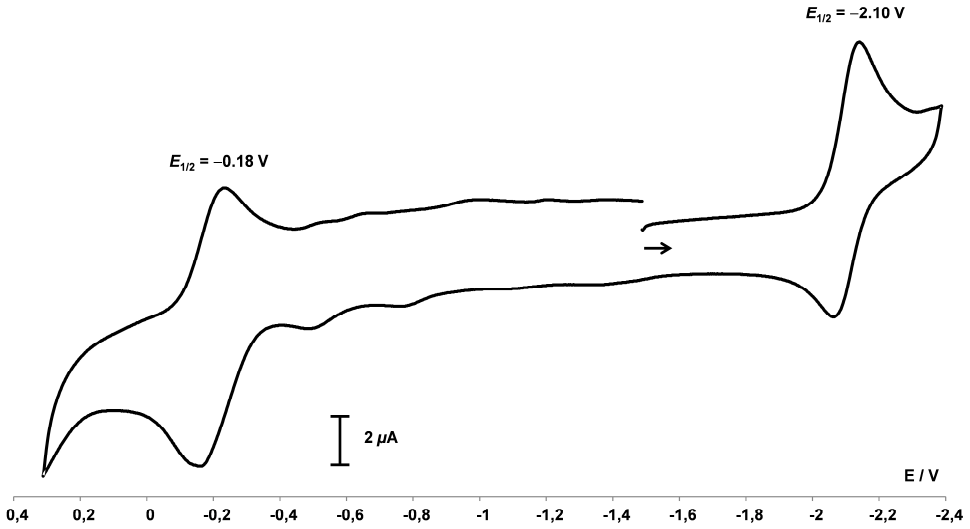

Figure 5S: Cyclic voltammogram of **14** (DMF, 0.1 M $[Bu_4N][PF_6]$, vs. FcH/FcH^+, 100 mV s^{-1}).

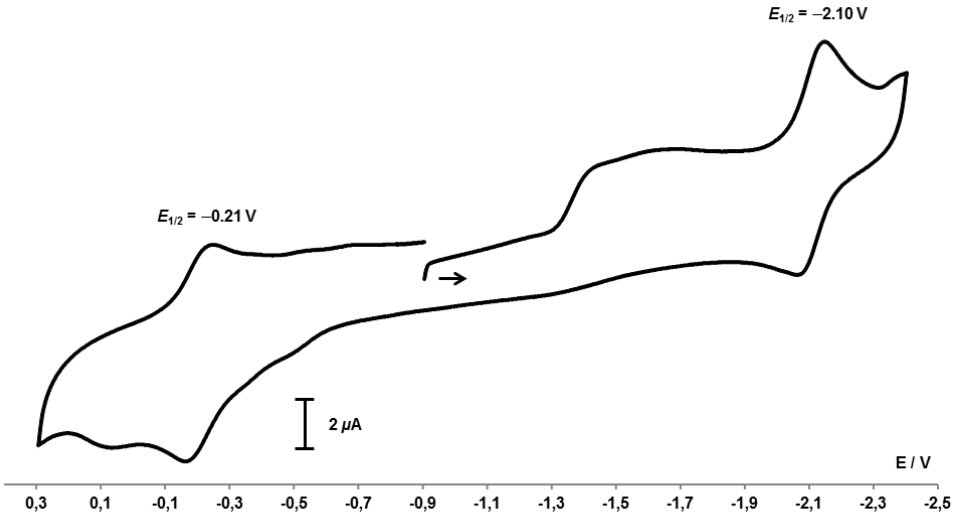

Figure 6S: Cyclic voltammogram of **16** (DMF, 0.1 M $[Bu_4N][PF_6]$, vs. FcH/FcH^+, 100 mV s^{-1}).